Molecular Crystals and Liquid Crystals
Publication details, including instructions for authors and subscription information:
http://www.tandfonline.com/loi/gmcl20

Polarization Ray Tracing in Twisted Liquid Crystal Systems

Gerben Boer [a] & Toralf Scharf [b]

[a] CSEM, Badenerstrasse 569, Zürich, CH-8048, Switzerland

[b] IMT, Breguet 2, Neuchâtel, CH-2000, Switzerland

Version of record first published: 18 Oct 2010

To cite this article: Gerben Boer & Toralf Scharf (2002): Polarization Ray Tracing in Twisted Liquid Crystal Systems, Molecular Crystals and Liquid Crystals, 375:1, 301-311

To link to this article: http://dx.doi.org/10.1080/713738376

Mol. Cryst. Liq. Cryst., Vol. 375, pp. 301-311

1058-725X/02 $12.00 + .00

Polarization Ray Tracing in Twisted Liquid Crystal Systems

GERBEN BOER[a] and TORALF SCHARF[b]

[a]*CSEM Badenerstrasse 569 CH-8048 Zürich, Switzerland and*
[b]*IMT Breguet 2 CH-2000 Neuchâtel, Switzerland*

In this paper it will be presented different ray trace models that are able to simulate uniaxial birefringent optical elements with twisted structure. There exist already methods to calculate the optical behavior of birefringent elements (including angular dependence) such as the Jones matrix method [2]. But those methods are not based on ray tracing and cannot be linked together with other optical components such as lenses for example. The aim of this work is to enable ray trace simulations of optical systems containing complex birefringent elements and extended sources. The developed models are applied on problems that are related to twist liquid crystal Wollaston prism.

Keywords ray-trace; polarization; simulation; twist nematic; birefringence; interferometry.

INTRODUCTION

To model systems incorporating birefringent elements, a ray trace program must take into consideration the polarization of light. So, two polarization components should be propagated through the system according the different refractive indices of the birefringent media they will encounter. The simulation of birefringent components with

uniform orientation is relatively simple but it becomes complex for twisted structures. The calculations of the optical transmission of twisted nematic cells are usually done with Jones matrix methods or a 4x4 matrix method (Berreman). These methods calculate accurately the angle-dependent phase retardation of two polarization components for planar systems but they don't give the spatial or directional separation between rays caused for instance by refraction at interfaces between anisotropic and isotropic materials. In our case of polarization interferometry with extended sources, the localization of the plane of interference is important. One finds this plane of localization of interference fringes as the point of intersection of beams that were split before. Since we need to perform ray-tracing simulations, a conventional matrix method is not suitable for our purpose. To overcome these problems, we developed new methods based on polarization ray tracing that can simulate twisted structures and take the direction of beams into account. We choose as a basis for our work the ray-trace program ASAP (Advanced Systems Analysis Program) form BRO [3]. This commercial available program is able to simulate accurately polarization properties of anisotropic uniaxial crystals as well as other conventional optical elements. We will present two different models for twisted elements. The first one is based on multiple ray-splitting. In the second one, the twisted cell is modeled in a similar way as in the Jones matrix calculus by using combinations of retarder plates and polarization rotators.

RAY TRACE IN UNIAXIAL MEDIA

In this chapter, we will discuss the possibility to simulate simple uniaxial birefringent component by splitting an incoming ray into an ordinary and extraordinary ray.

Each ray is characterized by the usual trace information such as ray direction, optical phase shift, flux and a polarization vector. When such a ray encounters uniaxial media, it splits into an ordinary and extraordinary ray. Snell's law gives the direction of these new rays. The reflection and transmission coefficients are calculated with the Fresnel formulae [4]. If one examines the case of a boundary between an isotropic material (index n) and an anisotropic material (index n_o and n_e), which is illustrated in Figure 1, the refraction angle ϕ_o for the ordinary ray is given by:

$$n \sin\phi = n_o \sin\phi_o \quad (1).$$

the refraction angle ϕ_e for the extraordinary ray is given by:

$$n \sin\phi = n_e(\phi_e) \sin\phi_e \quad (2)$$

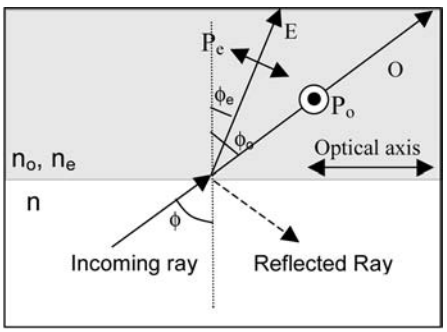

FIGURE. 1 Splitting at an isotropic anisotropic interface of an incoming ray into an ordinary (O) and extraordinary (E) ray.

The refractive index $n_e(\phi)$ depends on the angle of incidence ϕ and the orientation of the optical axis. The polarization vectors (P_o, P_e) attached to the ordinary and extraordinary rays are set perpendicular to the propagation direction. When passing through the crystal medium the ordinary ray will experience the refraction index n_o and the extraordinary ray will experience n_e. The two rays carry also their own optical path length and amplitude. The reflected part is not considered here and eventual multiple reflections are neglected.

ASAP uses this model for simulating simple uniaxial plates. In ASAP, each ray represents a Gaussian beam with a certain waist and divergence. An arbitrary field can be created by a judicious superposition of such Gaussian beams [7]. Those beams are then propagated by geometrical ray-trace methods [8]. Phase, amplitude and polarization state are changed accordingly to the birefringent components encountered by the rays. At the output (or at the detector), the different Gaussian beams can be added coherently (electric

amplitudes addition) or incoherently (square modulus of the electric field addition) with respect to each other.

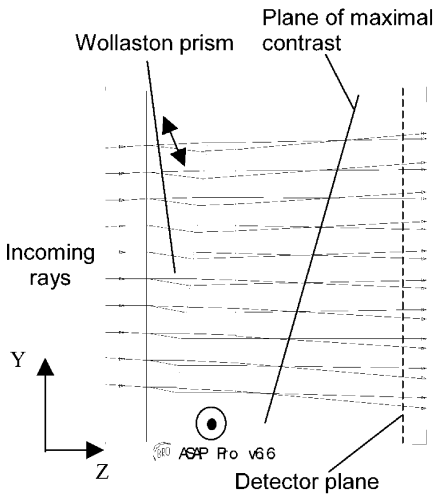

FIGURE 2 Ray tracing of a divergent source trough a Wollaston prism with tilted optical axis.

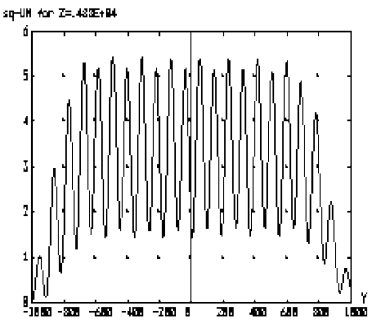

FIGURE 3 Interference pattern in the defocalised plane

Application to the Wollaston Prism

To show the performance of such ray trace method, we applied it to a polarization interferometer based on a Wollaston prism. As shown in Figure 2, a Wollaston prism consists of two wedges made of a birefringent material and joined by their hypotenuse. The optical axes are mutually perpendicular at the interface of the two wedges. If the Wollaston prism is placed between two linear polarizers at 45°, it becomes a polarization interferometer [5]. At the input of the Wollaston prism, the polarized light can be decomposed into two polarization components TE and TM. The TE component is parallel to the ordinary axis with index n_o and the TM component is parallel to the extraordinary axis with index n_e. In the second prism, the situation is inverted: TE and TM experience n_e and n_o respectively. By summing

the phase shift produced by each prism, the total phase difference δ between the two components at the output of the Wollaston becomes:

$$\delta = \frac{2\pi}{\lambda} 2y(n_e - n_o)\tan\theta, \tag{3}$$

where y is the vertical coordinate, λ the wavelength and θ the wedge angle. The light passes then through a second polarizer, which transforms this phase shift into an interference pattern (output interferogram). The Fourier-Transform of this interference pattern gives the spectrum of incident light [5].

One interesting property of interferometry is the localization of the plane of interference if extended sources are used. Actually, when an interferometer is illuminated by a spatially incoherent source, the interference fringes are localized in space [4]. Depending on the interferometer configuration, the localization of the fringes (or plane of maximal contrast) may be difficult to find.

To calculate the position of the plane of maximal contrast of the above-described interferometer, we need to simulate the directional changes of the rays. The interferometer was simulated with a spatial incoherent source by defining a set of point sources. Figure 2 gives a schematic overview: the incoming rays are split at the first interface due to the tilted optical axis and traverse the system. Behind the Wollaston prism, at the intersection point of the ordinary and extraordinary ray, one finds the locus of the plane of maximal contrast. Figure 3 shows the obtained interferogram for a detector plane that is defocalized as indicated in Figure 2. Because the detector plane is not the plane of maximal contrast, the contrast of the interferogram is only about 70%.

TWISTED STRUCTURES

In this previous chapter we have shown the possibilities to simulate optical systems containing simple uniaxial plates. Twisted structures are also interesting because of their numerous applications in liquid crystal devices. Angle dependence is one of the major problems when simulating such structures. Models that can calculate the transmission of light through birefringent media are the Jones Matrix or the Berreman method [2]. We will show here two different methods that have been implemented in ASAP to simulate twisted nematic (TN) cells.

Multiple Ray Splitting Method

In this first method, we divided the TN cell into N thin plates with linear increasing azimuthal angle of the optical axis. Each plate can be considered as a homogenous uniaxial media and it can be modeled as in the previous chapter. So, at the interface of each plate, all the rays are split into an ordinary and extraordinary ray and than propagated further. Finally, we end-up with considerable number of rays equal to 2^N rays because each incoming ray is split at each interface.

We applied this model to a system similar to the Wollaston prisms placed in between 45° polarizers. The birefringent homogenous prisms are replaced by wedge shaped twisted nematic cells as shown in Figure 4. For normal incidence, this configuration has the same optical properties as the classical Wollaston prism but the angular dependence is different.

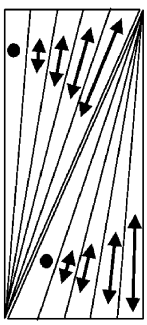

FIGURE 4 Wollaston prism made of two twisted nematic wedge cells.

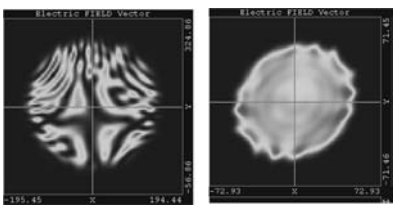

FIGURE 5 Interference pattern showing the field of view for (a) opposite twist sense configuration (b) equal twist configuration.

The angular dependence can be studied by focusing light (or rays) with high incidence angles into a point of interest. Since the number of rays needed to approximate accurately a converging wave front is proportional to the covered angle, we limit the incidence angles to the range of ±35°. The light is focused exactly in the center of the Wollaston prism (birefringence $\Delta n = 0.28$, wedge angle $\theta = 0.6°$ and thickness = 0.2 mm). We compare the field of view between two different configurations: the first configuration has two twisted nematic cells of opposite twist sense and the second configuration has

two twisted nematic cells with equal twist sense. The cells are divided into 7 slices each. Figure 5 (a) and (b) show the interference pattern in the far field for the configuration with opposite twist sense and equal twist sense respectively. In the angular range of ±35° the simulations are in accordance with experimental results given elsewhere [1]. Unfortunately, this method is suffering from the high computational times. As already mentioned above, the successive splitting produces a very high number of rays. Consequently, we have to limit the number of slices. Of course, this affects the quality of the simulation because the model becomes more precise with increasing number of slices. By using Fresnel formulas, losses due to simple reflections are taken into account but multiple reflections are not. So, this method is not suited to simulate twisted cells with high incidence angles where multiple reflections become important.

One splitting Ray Method

In a second approach, we model the cell as a set of polarization rotators and retarder plates. As shown in Figure 6, the cell is divided into N thin uniaxial crystal plates where each of them is followed by a polarization rotator. The azimuth angle of the optical axis of each plate is rotated by a constant amount with respect to the optical axis of the previous plate. The polarization rotators ($R(\phi/N)$) rotates the polarization vector attached to each ray by the same amount.

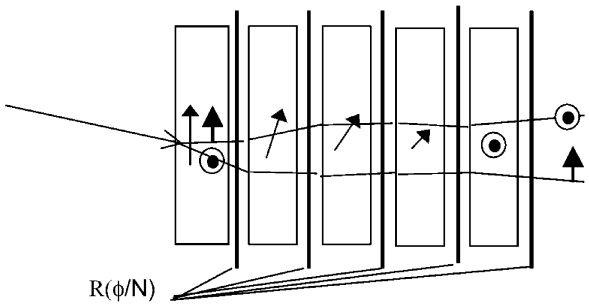

FIGURE 6 Ray tracing of an ordinary and extraordinary ray through a twisted nematic cell modeled with the one split algorithm.

At the first interface, the incoming rays are split into an ordinary and extraordinary ray. At the output of the first crystal plate the polarization vectors are rotated by ϕ/N with rotation matrices. At the entrance of the second plate, all rays are refracted. The polarization vector of the ordinary and extraordinary ray is projected parallel and perpendicular to the optical axis of the second plate. The same process is repeated for the following plates. Reflected light is not traced further, which causes problems for high angle of incidence. This algorithm doesn't takes multiple reflections into account but Fresnel [4] losses are considered. This ray trace algorithm is comparable to Jones matrix calculations because it divides the system into a set of retardation and rotation matrices [6]. However Jones matrix calculation does not takes the change of direction of the ordinary and extraordinary rays due to refraction into account.

In our model, the incoming rays are only split once at the first isotropic anisotropic interface. So, the number of rays at the output is reasonable and more complex simulations can be performed. In order to compare this new method with the previous one, we simulated the same configuration as shown in Figure 4. The system was illuminated with high angles of incidence up to ± 62°. Figures 7 (a) and (b) show the simulated field of view for configurations with opposite and equal twist sense respectively. Thanks to the reduced number of rays, the new method allows us to cover a much wider angular range (± 62°) than the simulations shown in Figure 5 (a) and (b). More accurate results for high incidence angles may be obtained with increasing number of layers per thickness.

For small angles of the liquid crystal wedge it is possible to regard the system as planar and one can simulate the angle dependence. Berreman matrix calculations with 100 layers are shown in Figure 7(c) and (d), which show a very large field of view for the configuration with equal twist sense. If one compares Figure 7 (a) and (b) with (c) and (d), the limitations of our model to small apertures becomes evident.

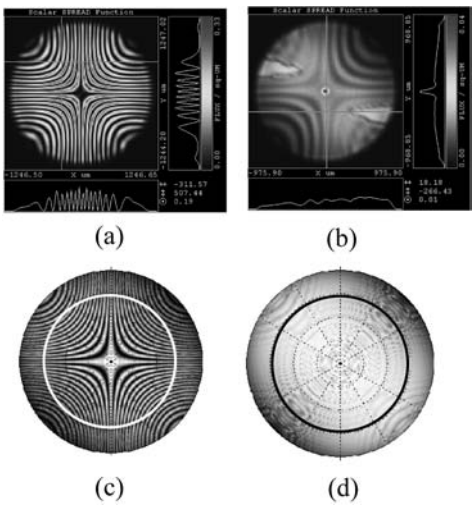

FIGURE. 7 Interference pattern showing the field of view: (a) opposite twist sense configuration, (b) equal twist sense configuration with 10 layers per cell, (c) Berreman calculation (100 layers) for the opposite twist,(d) Berreman calculation for the equal sense configuration. The white and black circles delimit the incidence angle within 60°.

In that what follows, we apply this method to find the plane of maximal contrast for the twisted configuration as we did before for the classical Wollaston prism (Figures 2 and 3). In this configuration, the plane of maximal contrast is located inside the Wollaston prism. For this reason, we used an additional lens in order to image the plane of maximal contrast on a detector plane. Figure 8(a) shows the ray tracing through the system. The extended source is simulated with the help of multiple monochromatic point sources (tree in Figure 8(a)), which are mutually incoherent.

The twisted cells that constitute the Wollaston prism are modeled as described in Figure 6. An ideal lens without aberrations images the interference pattern on the detector with a magnification of –1. We limit here the incidence angle to ± 4.5° so that internal reflections can be neglected. Figure 8(b) shows the obtained interferogram at the detector plane.

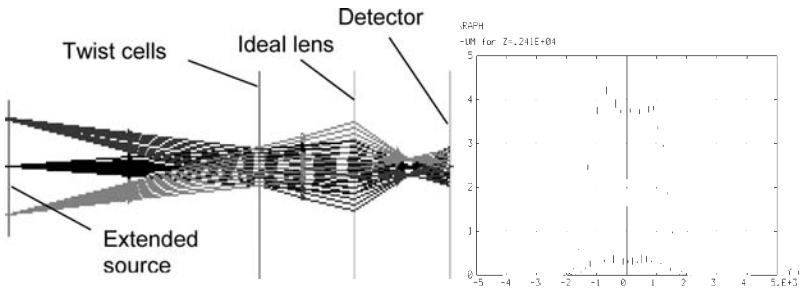

FIGURE 8 (a) Ray tracing with ASAP through a complete optical system. (b) Simulated interferogram at the detector plane.

CONCLUSION

We presented several methods able to simulate systems containing birefringent uniaxial materials and in particular twisted structures. Those methods are implemented in an optical ray trace program (ASAP), which enables us to simulate birefringent elements of almost any shape in combination with other optical elements, like lenses, mirrors or complete illumination systems. However, these methods are only suited for problems involving relatively thick twisted elements with small twist angles and limited incidence angles. The exact limitations of the presented methods have not yet been found.

REFERENCE

[1] G. Boer, T.Scharf, R.Dändliker, , submitted to Applied Optics.
[2] P. Yeh, and C. Gu, Optics of Liquid Crystal Displays (Wiley Interscience, New York, 1999).

[3] Breault Research Organization, "Polarization", (ASAP application notes, Tuscon, 1999)
[4] M. Born, and E. Wolf, Principles of Optics, sixth ed. (Cambridge university press,1980).
[5] M. J. Padgett, A. R. Harvey, A. J. Duncan, and W. Sibbett, Applied Optics **33** (25), 6035-6040 (1994).
[6] B. E. A.Saleh, M. C. Teich, Fundamentals of Photonics, (John Wiley, 1991). p.229.
[7] Breault Research Organization, "Wave optics", (ASAP application notes, Tuscon, 2001).
[8] J.Arnaud, Applied Optics **24** (4), 538-543 (1985).